A method of estimating the noise level in a chaotic time series

A. W. Jayawardena,[1,a)] Pengcheng Xu,[2] and W. K. Li[3]
[1]*International Centre for Water Hazard and Risk Management under the auspices of UNESCO, Public Works Research Institute, Tsukuba, Japan*
[2]*Academy of Mathematics and System Sciences, Chinese Academy of Sciences, Beijing, China*
[3]*Department of Statistics and Actuarial Sciences, The University of Hong Kong, Hong Kong, China*

(Received 13 June 2007; accepted 10 March 2008; published online 13 May 2008)

An attempt is made in this study to estimate the noise level present in a chaotic time series. This is achieved by employing a linear least-squares method that is based on the correlation integral form obtained by Diks in 1999. The effectiveness of the method is demonstrated using five artificial chaotic time series, the Hénon map, the Lorenz equation, the Duffing equation, the Rossler equation and the Chua's circuit whose dynamical characteristics are known *a priori*. Different levels of noise are added to the artificial chaotic time series and the estimated results indicate good performance of the proposed method. Finally, the proposed method is applied to estimate the noise level present in some real world data sets. © *2008 American Institute of Physics*. [DOI: 10.1063/1.2903757]

Almost all types of observed time series are contaminated with noise which may arise from a number of sources such as measurement errors, human errors, and transcribing errors. For many types of time series analysis, it is ideal, and sometimes necessary, to have data that are noise free. This is particularly so in the case of nonlinear time series, which have signatures of chaotic dynamics, because the techniques of analysis and prediction have been developed under the assumption that the series are noise free. In this paper, the authors present a method of estimating the noise level in a deterministic time series using a linear least-squares method. The method has been verified using known chaotic time series, and applied to some real world data series.

I. INTRODUCTION

Almost all types of observed time series are contaminated with noise that may arise from a number of sources such as measurement errors, human errors, and transcribing errors. For many types of time series analysis, it is ideal, and sometimes necessary, to have data which are noise free. This is particularly so in the case of nonlinear time series, which have signatures of chaotic dynamics, because the techniques of analysis and prediction have been developed under the assumption that the series are noise free. The presence of noise may limit the performance of the techniques of identification, estimation of invariant measures, model selection, and prediction of deterministic dynamical systems. For example, the presence of noise in the time series can destroy the self-similarity of the attractor, may distort the phase-space reconstruction and result in the prediction errors be bounded from below regardless of the prediction method used.

Because of the potential problems that could be encountered in the analysis and prediction processes, and the fact that noise is inherently present in almost all observational time series, the question of dealing with noise has attracted the attention of many investigators from different disciplines (Schreiber 1993a, 1993b; Diks 1999; Kantz and Schreiber 1997; Oltmans and Verheijen 1997; Jayawardena and Gurung 2000; among others). Attempts have been made to deal with the problem by noise reduction methods (e.g., Schreiber 1993b; Schreiber and Grassberger 1991; Grassberger *et al.* 1993), as well as by modifying the scaling law (Schouten *et al.* 1994). The verification of such methods can be carried out only for series in which the clean signal is known *a priori*. For practical time series, such methods are therefore not very useful. Alternatively, methods for determining the noise level have been proposed by Schreiber (1993a), Oltmans and Verheijen (1997), and Diks (1999), but their application is extremely difficult except in the limiting situations.

In this paper, the authors present a method of estimating the noise level in a deterministic time series using a linear least-squares method. The method is based on the correlation integral form obtained by Diks (1999) coupled with the special property of Kummer's confluent hypergeometric function. It is tested with five mathematical series, which are known to become chaotic under certain parameter conditions: the Hénon map, the Lorenz equation, the Duffing equation, the Rossler equation and the Chua's circuit. The tests show consistent satisfactory results. It is then applied to three real-world data series: the southern oscillation index (SOI), eastern equatorial Pacific sea surface temperature anomaly index (SSTA), and the normalized Darwin–Tahiti mean sea level pressure differences.

II. CORRELATION INTEGRAL

The first step in treating a time series as chaotic is to diagnose the system; i.e., to determine whether the time series is driven by a low dimensional deterministic system. It can be done by computing several invariant measures, such as the fractal dimension, the correlation dimension, the

[a)]Author to whom correspondence should be addressed. Electronic mail: hrecjaw@hkucc.hku.hk.

Lyapunov exponent, and the Kolmogorov entropy among others. Of these, the correlation dimension plays a significant role in identifying the system as well as for prediction of the future states of the system. For a deterministic time series generated by a dynamical system, the correlation integral $C_m(r)$, for small r and large m, is given by the scaling relationship,

$$C_m(r) \sim e^{-m\tau K} r^D, \tag{1}$$

where r is the radius, m is the embedding dimension, τ is the time delay, D is the correlation dimension, and K is the correlation entropy per time unit, or simply correlation entropy. The correlation dimension and the correlation entropy can respectively be interpreted as an approximate measure of the number of degrees of freedom, and a measure of the rate (T^{-1}) at which initially nearby orbits diverge.

The standard method of calculating the correlation integral is by the correlation sum method [Grassberger and Procaccia (1983a, 1983b)], as defined below:

$$C_m(r) = \frac{1}{N(N-1)} \sum_{i=1}^{N-1} \sum_{j=1}^{N} H(r - \|\boldsymbol{Y}_i - \boldsymbol{Y}_j\|), \quad i \neq j, \tag{2}$$

where H is the Heaviside step function with $H(u)=1$ for $u>0$, and $H(u)=0$ for $u \leqslant 0$; N is the number of points in the vector time series, $\boldsymbol{Y}_i$, $\boldsymbol{Y}_j$ are points in the reconstructed phase space; r is the radius of sphere centered on either of the points $\boldsymbol{Y}_i$, or $\boldsymbol{Y}_j$. A point in the phase space is defined as

$$\boldsymbol{Y}(t) = (x(t), x(t-\tau), \ldots, x(t-(m-1)\tau)), \tag{3}$$

where $x(t)$, $1 \leqslant t \leqslant N$ is a chaotic time series embedded in the reconstructed phase space of dimension m and time delay τ. The norm $\|\boldsymbol{Y}_i - \boldsymbol{Y}_j\|$ may be any one of the three usual norms, the maximum norm, the diamond norm, or the Euclidean norm. Correlation integrals are calculated for a series of embedding dimensions.

Equation (2), as well as other methods, is generally applicable to noise free time series. The presence of noise (dynamical and observational) strongly affects the correlation integral and the results may become distorted or even completely wrong. Several authors (for example, Ott and Hanson 1981; Ott *et al.* 1985; Smith 1992; Schreiber 1993a; Kantz and Schreiber 1997; Oltmans and Verheijen 1997; Diks 1999) have addressed the problem resulting from the presence of noise but it still remains a topic of current research interest.

A notable contribution on this topic is that of Schreiber (1993a), who obtained the following approximate formula based on the maximum norm for the correlation integral for a time series contaminated with Gaussian noise:

$$\frac{d[\ln(C_{m+1}(r))]}{d[\ln(r)]} = \frac{d[\ln(C_m(r))]}{d[\ln(r)]} + \frac{r \exp(-r^2/4\sigma^2)}{\sigma\sqrt{\pi}\,\mathrm{erf}(r/2\sigma)}, \tag{4}$$

where σ is the standard deviation of the Gaussian distribution, i.e., the noise level of the time series, and "erf" refers to the error function.

A more simple form for the correlation integral has been obtained by Schouten *et al.* (1994) also based on the maximum norm. Using an upper bound of radius r as r_0, and δ as the maximum noise amplitude, they obtained the correlation integral as

$$C_m(r) = \left[\frac{r-\delta}{r_0-\delta}\right]^D, \quad \text{for } \delta \leqslant r \leqslant r_0. \tag{5}$$

Subsequently, Diks (1999) derived the following expression for the correlation integral in the presence of noise when $C_m(r)$ is based on Euclidean norm:

$$C_m(r) = \frac{\phi e^{-m\tau K} m^{-D/2} 2^{-m} \sigma^{D-m} r^m}{\Gamma(m/2+1)} M\left(\frac{m-D}{2}, \frac{m}{2}+1, -\frac{r^2}{4\sigma^2}\right). \tag{6}$$

Diks' (1999) derivation is based on the closed form expression for the correlation integral in the presence of Gaussian noise obtained by Smith (1992) under the assumption that the clean attractor underlying the noisy data has an integer-valued dimension D, and a similar expression obtained by Oltmans and Verheijen (1997) under general conditions.

In Eq. (6), ϕ is a constant and M is Kummer's confluent hypergeometric function, which has the following integral representation:

$$M(a,b,z) = \frac{\Gamma(b)}{\Gamma(a)\Gamma(b-a)} \int_0^1 e^{zt} t^{a-1} (1-t)^{b-a-1} dt. \tag{7}$$

Using Eqs. (6) and (7), the correlation dimension and noise level for the time series can be estimated by a nonlinear least-squares method, at least in theory. However, because of the strong nonlinearity in the equations, it is difficult in practice.

III. NOISE LEVEL ESTIMATION

To overcome the difficulties involved in nonlinear least-squares method, a new method that employs a least-squares estimation procedure is introduced to estimate the correlation dimension and the noise level. Starting from Eqs. (6) and (7), a relationship linking the correlation dimension D, the correlation sum $C_m(r)$ with respect to r, and the noise level σ can be shown to be (see Appendix A for detailed derivation)

$$D + 2\left[m\frac{d[\ln(C_m(r))]}{d[\ln(r)]} - \frac{d^2[\ln(C_m(r))]}{d[\ln(r)]^2} - \left(\frac{d[\ln(C_m(r))]}{d[\ln(r)]}\right)^2\right]\frac{\sigma^2}{r^2} = \frac{d[\ln(C_m(r))]}{d[\ln(r)]}. \tag{8}$$

In this equation, the correlation dimension is linear with respect to σ^2. By substituting $\sigma=0$ in Eq. (8), the correlation dimension for noise free chaotic data can be obtained as

$$D = \frac{d[\ln C_m(r)]}{d[\ln r]}, \tag{9a}$$

and, for noisy data, as $r \to 0$, as (see Appendix B for proof)

$$\lim_{r\to 0} \frac{d[\ln C_m(r)]}{d[\ln r]} = m. \tag{9b}$$

Equation (8) can be rewritten in the form

$$y = D + 2\sigma^2 x, \tag{10a}$$

where

$$y = \frac{d[\ln C_m(r)]}{d[\ln r]}, \tag{10b}$$

$$x = \frac{1}{r^2}\left[m\frac{d[\ln C_m(r)]}{d[\ln r]} - \frac{d^2[\ln C_m(r)]}{(d[\ln r])^2} - \left(\frac{d[\ln C_m(r)]}{d[\ln r]}\right)^2\right], \tag{10c}$$

which, in their finite difference approximations take the form

$$y_n \approx r_n \frac{c_n - c_{n-1}}{\Delta r}, \tag{10d}$$

$$x_n \approx \frac{(m-1)\Delta r(c_n - c_{n-1}) - r_n(c_{n-1} - 2c_n + c_{n+1}) - r_n(c_n - c_{n-1})^2}{r_n(\Delta r)^2} \tag{10e}$$

for $r_{n+1} - r_n = \Delta r$; $c_n = \ln C_m(r_n)$, r_n, $1 \leqslant n \leqslant L$, a given radius, and L, the number of test values of the radius r.

The least-squares estimates of the noise level and the correlation dimension can then be shown to be

$$\bar{\sigma}^2 = \frac{\Sigma_{n=2}^{L-2}(y_{n+1} - y_n)(x_{n+1} - x_n)}{2\Sigma_{n=2}^{L-2}(x_{n+1} - x_n)^2}, \tag{11}$$

and

$$\bar{D} = \frac{1}{L-2}\sum_{n=2}^{L-1}(y_n - 2\bar{\sigma}^2 x_n). \tag{12}$$

IV. APPLICATION, RESULTS, AND DISCUSSION

The proposed approach is verified by using it to estimate the noise level of the following time series that are known to become chaotic under certain parameter and initial conditions, when known levels of noise are added.

Hénon map: The Hénon map (Hénon 1976) is given as

$$x_{n+1} = 1 - ax_n^2 + bx_{n-1} + n_n, \tag{13}$$

where n_n is a noise term and a and b are parameters. It has a chaotic attractor when $a=1.4$ and $b=0.3$ without noise.

Lorenz map: The Lorenz map (Lorenz 1963) is defined as

$$\frac{dx}{dt} = \sigma(y - x),$$

$$\frac{dy}{dt} = -xz + rx - y, \tag{14}$$

$$\frac{dz}{dt} = xy - bz.$$

It becomes chaotic for $\sigma=10$, $r=28$, and $b=8/3$.

Duffing equation: The Duffing equation (Ueda 1979) is defined as

$$\frac{dx}{dt} = y,$$

$$\frac{dy}{dt} = -ax - x^3 + b\cos(t), \tag{15}$$

and it becomes chaotic for $a=0.3$, $b=34.0$.

Rossler equation: Rossler equation (Rossler 1976) is defined as

$$\frac{dx}{dt} = -y - z,$$

$$\frac{dy}{dt} = x + ay, \tag{16}$$

$$\frac{dz}{dt} = b + z(x - c),$$

and it becomes chaotic for $a=0.15$, $b=0.2$, and $c=10$.

Chua's equation: Chua's circuit equation (Chua 1990; Elwalik and Kennedy 2000), is defined as

$$\frac{dx}{dt} = (1 - K - \varepsilon_r K)y - (1 + \varepsilon_r)x + \varepsilon_r z,$$

$$\frac{dy}{dt} = x + (K-2)y, \tag{17}$$

$$\varepsilon_c \frac{dz}{dt} = \varepsilon_r(x + Ky - z) - \alpha_1 z - \alpha_2(|z+1| - |z-1|),$$

and it becomes chaotic for $K=3.25$, $\varepsilon_r = 1/6$, $\varepsilon_c = 0.06$, $\alpha_1 = 0.8$, and $\alpha_2 = -0.5$.

The x_n values of the Hénon map are generated using Eq. (13) with $x_0=0.3$, $x_1=1.2$ and assuming n_n to be white noise ($n_n \sim N(0,\sigma)$) for $1 \leqslant n \leqslant 10\,000$. To ensure that the values of the time series are in the chaotic attractor, the first half of the generated series is discarded and a new series is formed using $s_n = x_{n+N}, 1 \leqslant n \leqslant 5000$ with $N=5000$. Equations

(14)–(17) have multispatial dimensions, and are solved numerically using the fourth-order Runge–Kutta method with a time step of 0.02 and initial conditions of

$$x_0 = 12.5, \quad y_0 = 2.5, \quad \text{and } z_0 = 1.5 \quad \text{for Eq. (14)},$$

$$x_0 = 0.1, \quad y_0 = 0.1 \quad \text{for Eq. (15)},$$

$$x_0 = 0.1, \quad y_0 = 0.1 \quad \text{and } z_0 = 0.1 \quad \text{for Eq. (16), and}$$

$$x_0 = 0.1, \quad y_0 = 0.1 \quad \text{and } z_0 = 0.1 \quad \text{for Eq. (17)}.$$

After obtaining the x component for each of the above equations [Eqs. (14)–(17)] for $x(t)$, $0 \leqslant t \leqslant 2000$ (a total of $(2000/0.02 = 100\,000)$ values will be generated), the discrete time series for subsequent analysis is obtained using the following equation and with a sampling interval of 10:

$$s_n = x(0.2n), \quad n > 0. \tag{18}$$

(Note that sampling interval × time step = 0.2.)

As before, out of the 10 000 values of the discrete time series s_n, only the second half is considered for further analysis. If different sampling intervals are used, different time series will be generated.

In order to embed the above time series into the phase space, the time delay and the embedding dimension must be given. For convenience, a time delay of unity is assumed for all the time series. A better choice for the embedding dimension is that in accordance with the embedding theorem of Takens (1981), which states that a D-dimensional attractor can be embedded into a $(2D+1)$-dimensional phase space, although other values could also be used. In this study, embedding dimensions of 5 and 7, respectively, are used for the Hénon series and other remaining series. Other values of embedding dimensions also lead to similar results.

Although the noise levels (σ) added to the artificial data sets generated by the above systems are known, the actual noise levels for the noisy data would be somewhat different. In this paper, the actual noise level is calculated as follows:

$$\sigma_{\text{Actual}} = \sqrt{\frac{1}{N-1}\sum_{i=1}^{N}(s_i - \bar{s}_i)^2}, \tag{19}$$

where N is the sample number, and $\{s_i, 1 \leqslant i \leqslant N\}$ and $\{\bar{s}_i, 1 \leqslant i \leqslant N\}$ are the noisy and clean data, respectively.

Figures 1–3, respectively, show the plots of $\ln(C_m(r))$ versus $\ln(r)$, the corresponding plots of $\boldsymbol{d}[\ln \boldsymbol{C_m}(\boldsymbol{r})]/\boldsymbol{d}[\ln \boldsymbol{r}]$ versus $\ln(r)$ and y versus x for all the data sets used in this study. The first five sets in each figure correspond to Hénon, Lorenz, Duffing, Rossler, and Chua series, for some selected values of added σ (The last three sets correspond to the real data sets). For the theoretical data sets, the relationships of $\ln(C_m(r))$ versus $\ln(r)$ are linear (or very near linear) when the data are noise free. They also show that the deviation from linearity increases as the noise level increases. The relationships $\boldsymbol{d}[\ln \boldsymbol{C_m}(\boldsymbol{r})]/\boldsymbol{d}[\ln \boldsymbol{r}]$ versus $\ln(r)$, show that the gradients of $\ln(C_m(r))$ versus $\ln(r)$ plots are independent (or almost independent) of $\ln(r)$ for clean data (except for Duffing data, which give a slight deviation from the rest), whereas some scaling regions where the variations are smooth can be identified for noisy data. These scaling regions are different for different values of added noise levels. They would provide more precise information for the correlation integral, and, could therefore be used to estimate the noise level.

The (x,y) plots (Fig. 3) for Hénon, Lorenz, Duffing, Rossler, and Chua series in the neighborhood of the scaling regions for selected values of the added noise level σ show that all the plots are concentrated around straight lines whose slopes enable the estimation of the noise levels. It can also be seen that the points are closer to the straight lines for lower values of σ and the spread increases as the noise level increases. Table I gives the comparisons of the added, actual and estimated noise levels by the proposal method and by Schreiber's method (Schreiber 1993a) together with the differences in the estimates of noise level by the proposed method and the added noise level, the differences between the noise levels estimated by Schreiber's method and the added noise level, the differences between the noise levels estimated by the proposed method and the actual noise level, and the differences in the noise levels estimated by Schreiber's method and the actual noise level. For almost all the results (13 out of 15 cases for the actual noise levels and the added noise levels), the comparisons consistently show that the noise levels estimated by the proposed method are closer to both the added noise levels and the actual noise levels [Eq. (19)] than those estimated by Schreiber's method. The corresponding standard errors between estimated and added (or actual) noise are given in Table II, which also consistently shows that the standard errors for the added and actual noise are always lower by the proposed method than those by Schreiber's method. The standard errors should however be interpreted with caution because the sample size is only 3. In fact they are slightly more closer to the actual noise levels than to the added noise levels. It should also be noted that the proposed method has the advantage that it is linear, whereas Schreiber's method is nonlinear.

The estimation of (x_n, y_n) in Eqs. (10d) and (10e) depends heavily on $C_m(r_n)$, which in turn depends on r, that should not be too small or too large. Although the curves of $\boldsymbol{d}[\ln \boldsymbol{C_m}(\boldsymbol{r})]/\boldsymbol{d}[\ln \boldsymbol{r}]$ versus $\ln(r)$ look noisy, there still exist some intervals where the slope change is relatively smooth. Such intervals (for $r = 0.1-0.3$) are used for the calculation of (x_n, y_n). The noise levels added are not insignificant (signal-to-noise ratio ranging from about 11 to 28), but not large enough to overshadow the signal.

The last three sets of graphs in Figs. 1–3 correspond to three real-world time series, all of which are related to a phenomenon known as El Nino and Southern Oscillation (ENSO), which leads to abnormal weather patterns around the globe. The occurrence of ENSO is characterized by two indices known, respectively, as the southern oscillation index (SOI), which is a normalized Darwin–Tahiti sea level pressure difference, and the eastern equatorial Pacific sea surface temperature anomaly (SSTA) index. Sustained negative values of SOI are accompanied by weak Pacific trade winds, reduced rainfall over eastern and northern Australia, and warming of the central and eastern tropical Pacific oceans. On the other hand, sustained positive values bring about

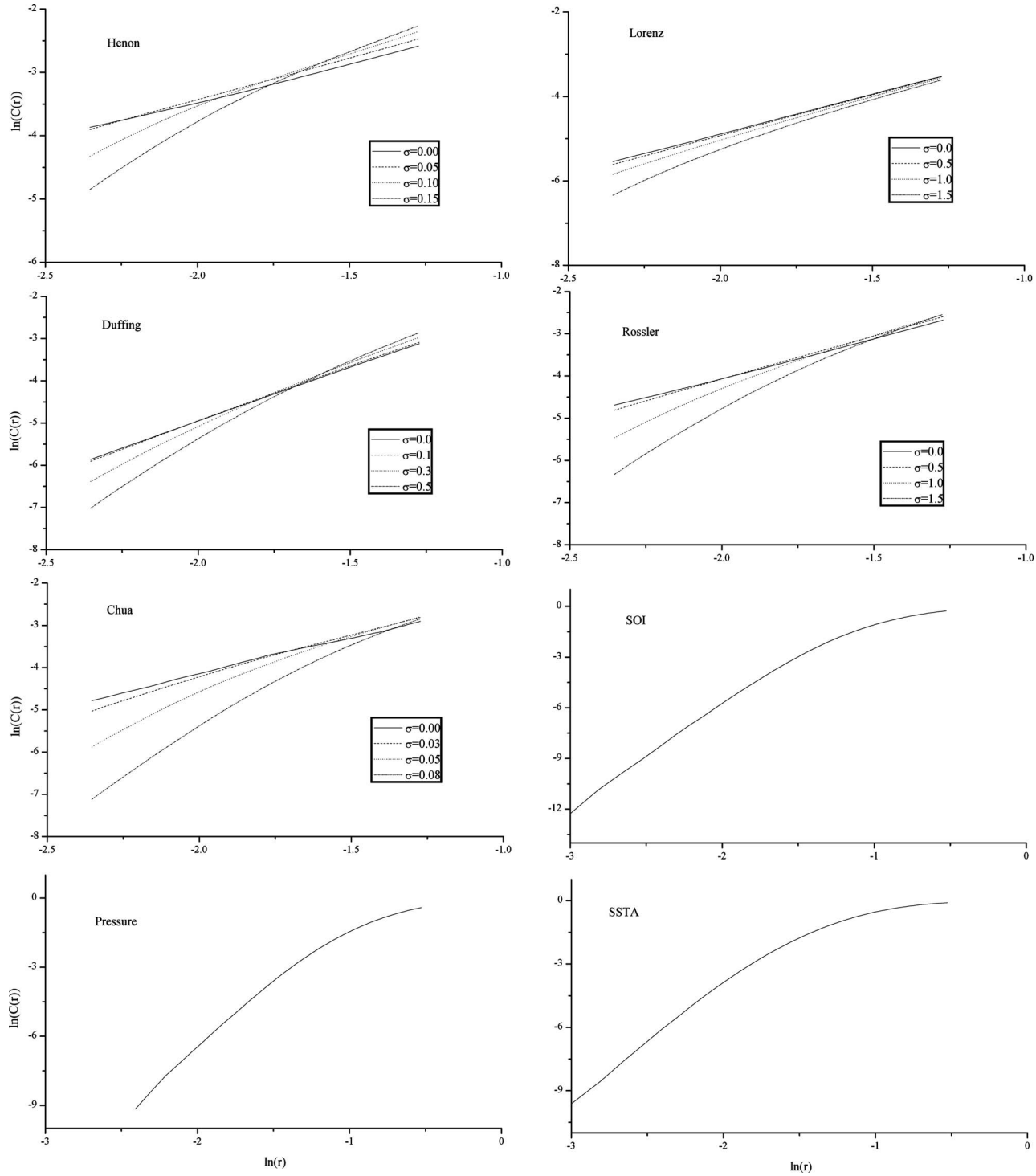

FIG. 1. Plots of $\ln(C(r))$ vs $\ln(r)$ for all the data sets used in this study. The first five sets correspond to Hénon, Lorenz, Duffing, Rossler, and Chua series for some selected values of added noise; the last three sets correspond to three real-world time series.

strong Pacific trade winds, wetter than normal rainfalls in eastern and northern Australia, and cooler sea surface temperatures in central and eastern Pacific oceans. Sustained negative values of SOI correspond to El Nino events whereas sustained positive values correspond to La Nina events. The second index, SSTA, averaged over the region 6N–6S°, 180–90W° is also called the cold tongue index, and is widely used to describe the occurrence of El Nino and La Nina. The third data set used is another version of the normalized Darwin–Tahiti sea level pressure difference but used to characterize the same phenomenon. The differences in the three data sets arise from the way they are averaged, normalized and the periods of record. SOI data are for the period January 1876 to December 2006, SSTA for the period January 1893 to December 1998 and the last data set for the period from January 1876 to December 1998. All data sets are given as monthly averaged values and are available in public domains in a number of web sites (see, e.g., http://www.bom.gov.au).

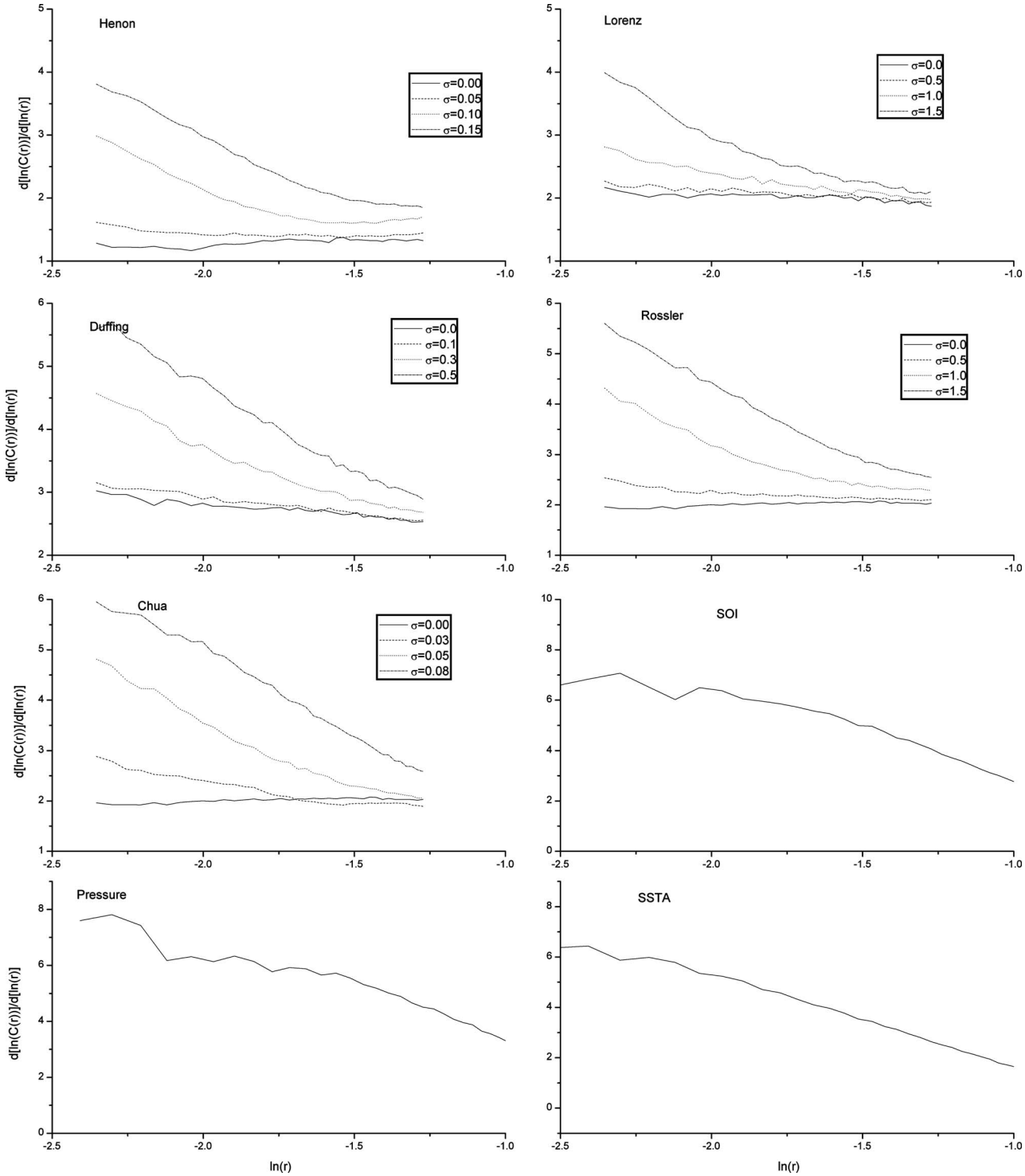

FIG. 2. Plots of $d[\ln(C(r))]/d[\ln(r)]$ vs $\ln(r)$ for all the data sets used in this study. The first five sets correspond to Hénon, Lorenz, Duffing, Rossler, and Chua series for some selected values of added noise; the last three sets correspond to three real-world time series.

The noise levels for the SOI, sea surface temperature anomaly index, and the sea level pressure differences are, respectively, 1.21, 3.13, and 1.26, and the corresponding correlation dimensions are 0.8015, 0.4575, and 0.9926. Although these results cannot be verified, it is reasonable to expect them to be acceptable since the method has been extensively verified using several examples.

V. CONCLUDING REMARKS

In this study, a method of estimating the noise level present in a chaotic time series is proposed by employing the linear least-squares method. This is an improvement over previous methods of estimating the noise level all of which use the nonlinear least squares method. In the present method, a linear form connecting the correlation sum, the

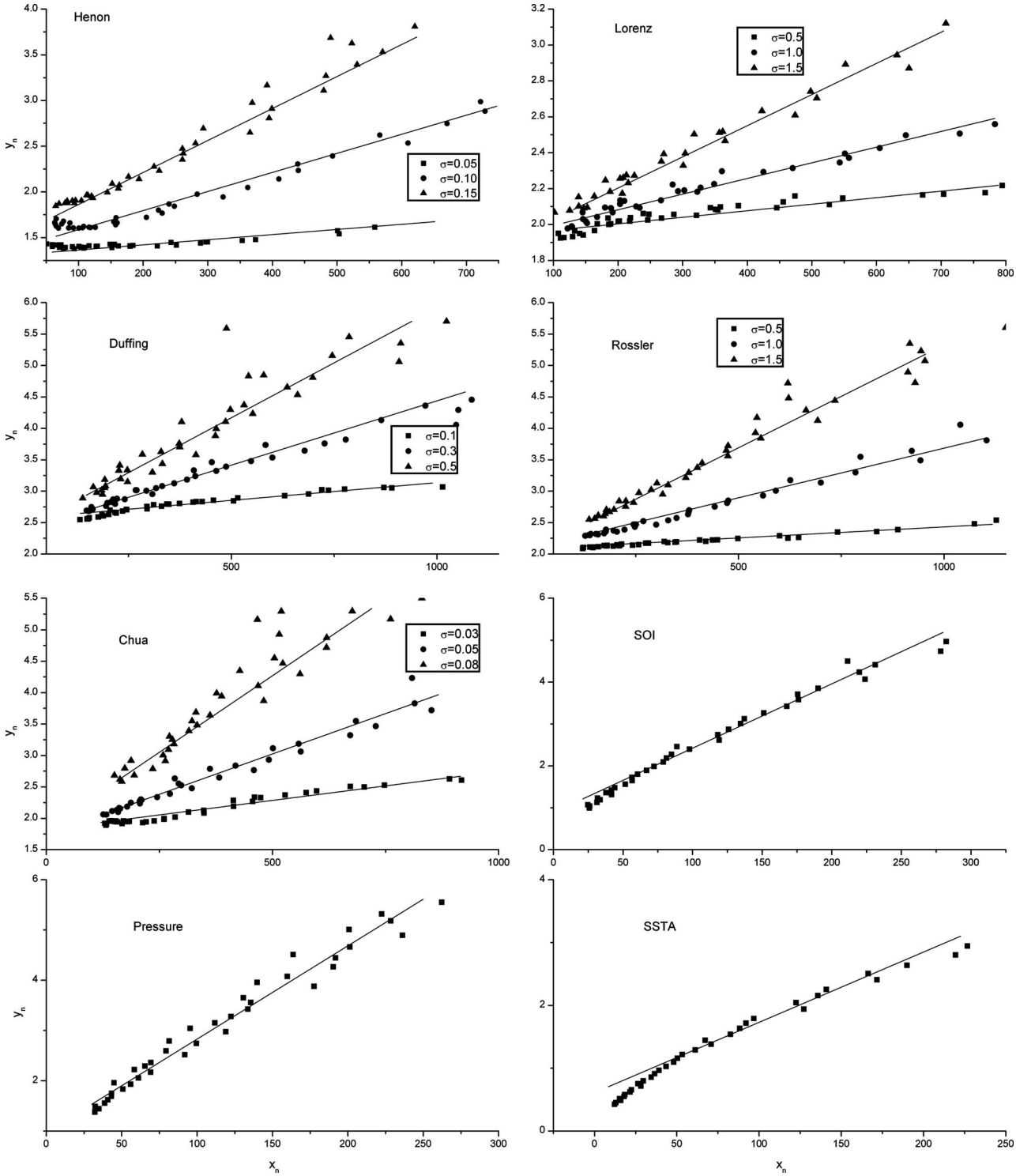

FIG. 3. Plots of y_n vs x_n [Eq. (12)] for all the data sets used in this study. The first five sets correspond to Hénon, Lorenz, Duffing, Rossler, and Chua series for some selected values of added noise; the last three sets correspond to three real-world time series.

noise level and the correlation dimension is obtained. It is easier to apply and is expected to lead to less computing error compared to a nonlinear method. The method is verified using some artificial chaotic time series generated by Hénon map, Lorenz equation, Duffing's equation, Rossler equation, and Chua's equation with added Gaussian noise. The numerical results consistently show that the proposal method give better estimates of the noise level for these chaotic time series than those obtained by the nonlinear method introduced by Schreiber (1993a, 1993b). The application part includes noise level estimations of monthly SOI, monthly eastern equatorial Pacific sea surface anomaly index, and normalized monthly Darwin–Tahiti sea level pressure differences.

TABLE I. Comparison of noise levels. σ—Added noise level; σ_{actual}—Actual noise level; $\hat{\sigma}$—Estimated noise level by the proposed method; $\hat{\sigma}_{\text{Schreiber}}$—Estimated noise level by Schreiber's method; SNR—Signal-to-noise ratio.

Data set	Hénon			Lorenz			Duffing			Rossler			Chua		
σ	0.05	0.10	0.15	0.5	1.0	1.5	0.1	0.3	0.5	0.5	1.0	1.5	0.03	0.05	0.08
σ_{actual}	0.0500	0.1004	0.1506	0.5020	1.0039	1.5059	0.1004	0.3012	0.5020	0.5020	1.0039	1.5059	0.0301	0.0502	0.0803
SNR	23.148	17.190	13.771	27.977	21.983	18.502	28.350	18.849	14.503	24.054	18.077	14.632	19.664	15.310	11.423
$\hat{\sigma}$	0.0360	0.0967	0.1468	0.7527	1.1391	1.6336	0.1897	0.3556	0.5370	0.4670	1.0119	1.5093	0.0297	0.0505	0.0793
$\hat{\sigma}_{\text{Schreiber}}$	0.0860	0.0711	0.0798	2.5115	2.0475	1.4306	0.2438	0.2756	0.3046	0.6360	0.8245	0.8986	0.0492	0.0474	0.0397
$\hat{\sigma}-\sigma$	−0.014	−0.0033	−0.0032	0.2527	0.1391	0.1336	0.0897	0.0556	0.037	−0.033	0.0119	0.0093	−0.0003	0.0005	−0.0007
$\hat{\sigma}_{\text{Schreiber}}-\sigma$	0.0360	−0.0289	−0.0702	2.0115	1.0475	−0.0694	0.1438	−0.0244	−0.1954	0.1360	−0.1755	−0.6014	0.0192	−0.0026	−0.0403
$\hat{\sigma}-\sigma_{\text{actual}}$	−0.014	−0.0037	−0.0038	0.2507	0.1352	0.1277	0.0893	0.0544	0.035	−0.035	0.008	0.0034	−0.0004	0.0003	−0.001
$\hat{\sigma}_{\text{Schreiber}}-\sigma_{\text{actual}}$	0.0360	−0.0293	−0.0708	2.0095	1.0436	−0.0753	0.1434	−0.0256	−0.1974	0.1340	−0.1794	−0.6073	0.0191	−0.0028	−0.0406

ACKNOWLEDGMENTS

The work presented in this paper, partially supported by the Hong Kong Research Grants Council Grant No. 7003/97E, was initially carried out while the first author was attached to the Department of Civil Engineering, The University of Hong Kong, and the second author was visiting. The work was also partially supported by a grant from the University Grants Committee of the Hong Kong Special Administrative Region, China (Project No. AoE/P-04/04). The authors also thank the anonymous reviewers whose critical comments made improvements to the original manuscript possible.

APPENDIX A: DERIVATION OF EQ. (8)

With the substitution of

$$a=\frac{m-D}{2},\quad b=\frac{m}{2}+1,\quad z=-\frac{r^2}{4\sigma^2} \tag{A1}$$

in Kummer's confluent hypergeometric function [Eq. (7)], Eq. (6) can be rewritten as

$$\begin{aligned} C_m(r) &= \frac{\phi e^{-m\tau K} m^{-D/2} 2^{-m} \sigma^{D-m} r^m}{\Gamma(m/2+1)} M\left(\frac{m-D}{2}, \frac{m}{2}+1; -\frac{r^2}{4\sigma^2}\right) \\ &= \frac{\phi e^{-m\tau K} m^{-D/2} 2^{-m} \sigma^{D-m} r^m}{\Gamma(m/2+1)} \frac{\Gamma(m/2+1)}{\Gamma((m-D)/2)\Gamma(D/2+1)} F\left(-\frac{r^2}{4\sigma^2}\right) = \frac{\phi e^{-m\tau K} m^{-D/2} 2^{-m} \sigma^{D-m} r^m}{\Gamma(D/2+1)\Gamma((m-D)/2)} F\left(-\frac{r^2}{4\sigma^2}\right), \end{aligned} \tag{A2}$$

where

$$F(z)=\int_0^1 e^{zt} t^{a-1}(1-t)^{b-a-1} dt. \tag{A3}$$

It can be proved that Eq. (A3) satisfies the condition

$$aF(z)+(z-b)F'(z)-zF''(z)=0 \tag{A4}$$

(see Appendix C for the proof).

Taking natural logarithms of Eq. (A2),

$$\begin{aligned} \ln[C_m(r)] = \ln(\phi) - \frac{D}{2}\ln(m) - m\ln(2) + (D-m)\ln(\sigma) \\ + m\ln(r) - m\tau K + \ln[(F)] - \ln\left[\Gamma\left(\frac{D}{2}+1\right)\right] \\ - \ln\left[\Gamma\left(\frac{m-D}{2}\right)\right]. \end{aligned} \tag{A5}$$

From Eq. (A1), we have

TABLE II. Standard errors between estimated and added (or actual) noise for the data sets.

	Added noise		Actual noise	
Data set	Proposed method	Schreiber's method	Proposed method	Schreiber's method
Hénon	0.010 42	0.059 41	0.010 59	0.059 86
Lorenz	0.224 8	1.604 4	0.220 7	1.602 0
Duffing	0.079 08	0.172 4	0.077 97	0.173 2
Rossler	0.025 66	0.453 3	0.025 50	0.457 7
Chua	0.000 644 2	0.031 62	0.000 790 6	0.031 79

$$\frac{dz}{dr} = -\frac{r}{2\sigma^2}. \tag{A6}$$

Since all the terms in Eq. (A5), except $\ln[C_m(r)]$, $m\ln(r)$ and $\ln[F(z)]$, are independent of r, their derivatives with respect to r are zero. Therefore,

$$\frac{d[\ln(C_m(r))]}{dr} = \frac{d}{dr}[m\ln(r) + \ln(F(z))] = \frac{m}{r} + \frac{1}{F(z)}\frac{d}{dr}(F(z)) = \frac{m}{r} - \frac{r}{2\sigma^2}\frac{F'(z)}{F(z)}, \tag{A7}$$

from which

$$\frac{F'(z)}{F(z)} = 2\sigma^2\left(\frac{m}{r^2} - \frac{d[\ln(C_m(r))]}{rdr}\right)$$

denote

$$P(m,r) = \frac{m}{r^2} - \frac{d[\ln(C_m(r))]}{rdr}.$$

Then,

$$F'(z) = 2\sigma^2 P(m,r)F(z). \tag{A8}$$

In addition,

$$\frac{d}{dr}(F'(z)) = F''(z)\frac{dz}{dr} = -\frac{r}{2\sigma^2}F''(z)$$

and

$$\frac{d}{dr}(F'(z)) = \frac{d}{dr}[2\sigma^2 P(m,r)F(z)] = 2\sigma^2\left\{F(z)\frac{dP(m,r)}{dr} + P(m,r)\frac{dF(z)}{dr}\right\} = 2\sigma^2\left\{F(z)\frac{dP(m,r)}{dr} - \frac{r}{2\sigma^2}F'(z)P(m,r)\right\}$$
$$= 2\sigma^2\left\{F(z)\frac{dP(m,r)}{dr} - \frac{r}{2\sigma^2}[2\sigma^2 P(m,r)F(z)]P(m,r)\right\} = 2\sigma^2\left\{F(z)\frac{dP(m,r)}{dr} - rP^2(m,r)F(z)\right\}.$$

Therefore,

$$F''(z) = -\frac{2\sigma^2}{r}\frac{d}{dr}(F'(z)) = -\frac{2\sigma^2}{r}\left\{2\sigma^2\left[\frac{dP(m,r)}{dr}F(z) - rP^2(m,r)F(z)\right]\right\} = -4\sigma^4\left\{\frac{dP(m,r)}{rdr} - P^2(m,r)\right\}F(z). \tag{A9}$$

Substituting Eqs. (A8) and (A9) and into Eq. (A4), we get

$$\boldsymbol{aF}(z) + (z-\boldsymbol{b})[2\boldsymbol{\sigma}^2\boldsymbol{P}(\boldsymbol{m},\boldsymbol{r})\boldsymbol{F}(z)] + 4\boldsymbol{\sigma}^4 z\left\{\frac{\boldsymbol{dP}(\boldsymbol{m},\boldsymbol{r})}{\boldsymbol{rdr}} - \boldsymbol{P}^2(\boldsymbol{m},\boldsymbol{r})\right\}\boldsymbol{F}(z) = 0,$$

which leads to

$$a + 2\sigma^2(z-b)P(m,r) + 4z\sigma^4\left\{\frac{dP(m,r)}{rdr} - P^2(m,r)\right\} = 0.$$

Then,

$$a - 2\sigma^2\left(\frac{r^2}{4\sigma^2} + b\right)P(m,r) - r^2\sigma^2\left\{\frac{dP(m,r)}{rdr} - P^2(m,r)\right\} = 0. \tag{A10}$$

Since $a=(m-D)/2$, $b=m/2+1$, we have

$$\frac{m-D}{2} - 2\sigma^2\left(\frac{r^2}{4\sigma^2} + \frac{m}{2} + 1\right)P(m,r) - \sigma^2\left[\frac{rdP(m,r)}{dr} - r^2P^2(m,r)\right] = 0.$$

Therefore,

$$\frac{m-D}{2} - \left[\frac{r^2}{2} + \sigma^2(m+2)\right]P(m,r) - \sigma^2\left[\frac{rdP(m,r)}{dr} - r^2P^2(m,r)\right] = 0$$

and

$$m - D - r^2P(m,r) - 2\sigma^2(m+2)P(m,r) - 2\sigma^2\frac{rdP(m,r)}{dr} + 2\sigma^2r^2P^2(m,r) = 0.$$

Thus, we have

$$m - r^2P(m,r) = D + 2\sigma^2\left\{(m+2)P(m,r) + \frac{rdP(m,r)}{dr} - r^2P^2(m,r)\right\}. \tag{A11}$$

Because

$$P(m,r) = \frac{m}{r^2} - \frac{d[\ln(C_m(r))]}{rdr}, \tag{A12}$$

we have

$$\frac{dP(m,r)}{dr} = -\frac{2m}{r^3} + \frac{1}{r^2}\frac{d[\ln(C_m(r))]}{dr} - \frac{1}{r}\frac{d^2[\ln(C_m(r))]}{dr^2} \tag{A13}$$

and

$$P^2(m,r) = \frac{m^2}{r^4} - \frac{2m}{r^3}\frac{d[\ln(C_m(r))]}{dr} + \frac{1}{r^2}\left[\frac{d[\ln(C_m(r))]}{dr}\right]^2. \tag{A14}$$

By substituting Eqs. (A12)–(A14) into Eq. (A11), we obtain

$$\begin{aligned} m - r^2P(m,r) &= D + 2\sigma^2\left\{\frac{m(m+2)}{r^2} - \frac{(m+2)}{r}\frac{d[\ln(C_m(r))]}{dr} - \frac{2m}{r^2} + \frac{1}{r}\frac{d[\ln(C_m(r))]}{dr} - \frac{d^2[\ln(C_m(r))]}{dr^2} - \frac{m^2}{r^2}\right. \\ &\quad \left. + \frac{2m}{r}\frac{d[\ln(C_m(r))]}{dr} - \left[\frac{d[\ln(C_m(r))]}{dr}\right]^2\right\} \\ &= D + 2\sigma^2\left\{\frac{(m-1)}{r}\frac{d[\ln(C_m(r))]}{dr} - \frac{d^2[\ln(C_m(r))]}{dr^2} - \left[\frac{d[\ln(C_m(r))]}{dr}\right]^2\right\} \\ &= D + \frac{2\sigma^2}{r^2}\left\{(m-1)r\frac{d[\ln(C_m(r))]}{dr} - r^2\frac{d^2[\ln(C_m(r))]}{dr^2} - r^2\left[\frac{d[\ln(C_m(r))]}{dr}\right]^2\right\}. \end{aligned}$$

However,

$$m - r^2P(m,r) = \frac{d[\ln(C_m(r))]}{d[\ln(r)]}$$

and

$$\begin{aligned} &r\frac{d[\ln(C_m(r))]}{dr} + r^2\frac{d}{dr}\left[\frac{d[\ln(C_m(r))]}{dr}\right] \\ &= r\frac{d}{dr}\left[r\frac{d[\ln(C_m(r))]}{dr}\right] = \frac{d}{d[\ln(r)]}\left[\frac{d[\ln(C_m(r))]}{d[\ln(r)]}\right] \\ &= \frac{d^2[\ln(C_m(r))]}{d[\ln(r)]^2}. \end{aligned}$$

Therefore,

$$D + 2\left[m\frac{d[\ln(C_m(r))]}{d[\ln(r)]} - \frac{d^2[\ln(C_m(r))]}{d[\ln(r)]^2} - \left(\frac{d[\ln(C_m(r))]}{d[\ln(r)]}\right)^2\right]\frac{\sigma^2}{r^2} = \frac{d[\ln(C_m(r))]}{d[\ln(r)]}. \tag{8'}$$

APPENDIX B: PROOF OF EQ. (9b)

For noisy data, from Eq. (A7),

$$\frac{d[\ln(C_m(r))]}{rdr} = \frac{m}{r^2} - \frac{1}{2\sigma^2}\frac{F'(z)}{F(z)},$$

$$\frac{d[\ln(C_m(r))]}{d[\ln(r)]} = m - \frac{r^2}{2\sigma^2}\frac{F'(z)}{F(z)}.$$

Because $F(z), F'(z)$ are bounded for $z \to 0$,

$$\lim_{r\to 0}\frac{d[\ln C_m(r)]}{d[\ln r]} = m. \tag{9b'}$$

APPENDIX C: PROOF OF EQ. (A4)

Kummer's confluent hypergeometric function has the integral representation:

$$M(a,b,z) = \frac{\Gamma(b)}{\Gamma(a)\Gamma(b-a)}\int_0^1 e^{zt}t^{a-1}(1-t)^{b-a-1}dt. \tag{C1}$$

First, let

$$F(z) = \int_0^1 e^{zt}t^{a-1}(1-t)^{b-a-1}dt. \tag{C2}$$

Then,

$$\begin{aligned} F'(z) &= \int_0^1 e^{zt}t^{a}(1-t)^{b-a-1}dt, \\ F''(z) &= \int_0^1 e^{zt}t^{a+1}(1-t)^{b-a-1}dt. \end{aligned} \tag{C3}$$

We have

$$\int_0^1 e^{zt}t^{a}(1-t)^{b-a-1}dt = -\frac{1}{b-a}\int_0^1 e^{zt}t^{a}d[(1-t)^{b-a}]. \tag{C4}$$

By using integration by parts, Eq. (C4) is

$$\int_0^1 e^{zt}t^a(1-t)^{b-a-1}dt = \frac{z}{b-a}\int_0^1 e^{zt}t^a(1-t)^{b-a}dt + \frac{a}{b-a}\int_0^1 e^{zt}t^{a-1}(1-t)^{b-a}dt$$

$$= \frac{z}{b-a}\int_0^1 e^{zt}t^a(1-t)(1-t)^{b-a-1}dt + \frac{a}{b-a}\int_0^1 e^{zt}t^{a-1}(1-t)(1-t)^{b-a-1}dt$$

$$= \frac{z}{b-a}\left[\int_0^1 e^{zt}t^a(1-t)^{b-a-1}dt - \int_0^1 e^{zt}t^{a+1}(1-t)^{b-a-1}dt\right]$$

$$+ \frac{a}{b-a}\left[\int_0^1 e^{zt}t^{a-1}(1-t)^{b-a-1}dt - \int_0^1 e^{zt}t^a(1-t)^{b-a-1}dt\right]$$

$$= \frac{z}{b-a}[F'(z) - F''(z)] + \frac{a}{b-a}[F(z) - F'(z)].$$

We then have

$$aF(z) + (z-b)F'(z) - zF''(z) = 0. \qquad (A4')$$

Chua, L. O. and Lin, G., "Canonical realization of Chua's circuit family," IEEE Trans. Circuits Syst. **37**, 885 (1990).

Diks, C., *Nonlinear Time Series Analysis, Methods and Applications* (World Scientific, Singapore, 1999).

Diks, C., Zwet, W. R., van Takens, F., and DeGoede, J., "Detecting differences between delay vector distributions," Phys. Rev. E **53**, 2169 (1996).

Elwalik, A. S. and Kennedy, M. P., "Chua's circuit decomposition: a systematic design approach for chaotic oscillators," J. Franklin Inst. **337**, 251 (2000).

Grassberger, P., Hegger, R., Kantz, H., Schaffrath, C., and Schreiber, T., "On noise reduction methods for chaotic data," Chaos **3**, 127 (1993).

Grassberger, P. and Procaccia, I., "Measuring the strangeness of strange attractors," Physica D **9**, 189 (1983a).

Grassberger, P. and Procaccia, I., "Generalized dimensions of strange attractors," Phys. Lett. **97A**, 227 (1983b).

Hénon, M., "A two-dimensional mapping with a strange attractor," Commun. Math. Phys. **50**, 69 (1976).

Jayawardena, A. W. and Gurung, A. B., "Noise reduction and prediction of hydrometeorological time series: dynamical systems approach vs. stochastic approach," J. Hydrol. **228**, 242 (2000).

Kantz, H. and Schreiber, T., *Nonlinear Time Series Analysis* (Cambridge University Press Cambridge, 1997).

Lorenz, E. N., "Deterministic non-periodic flow," J. Atmos. Sci. **20**, 130 (1963).

Oltmans, H. and Verheijen, P. J. T., "Influence of noise on power-law scaling functions and an algorithm for dimension estimations," Phys. Rev. E **56**, 1160 (1997).

Ott, E. and Hanson, J. D., "The effect of noise on the structure of strange attractors," Phys. Lett. **85A**, 20 (1981).

Ott, E., Yorke, E. D., and Yorke, J. A., "A scaling law. How an attractor's volume depends on noise level," Physica D **16**, 62 (1985).

Rossler, O. E., "An equation for continuous chaos," Phys. Lett. **57A**, 397 (1976).

Schouten, J. C., Takens, F., and van den Bleek, C. M., "Estimation of the dimension of a noisy attractor," Phys. Rev. E **50**, 1851 (1994).

Schreiber, T., "Determination of the noise level of chaotic time series," Phys. Rev. E **48**, R13 (1993a).

Schreiber, T., "Extremely simple noise reduction method," Phys. Rev. E **47**, 2401 (1993b).

Schreiber, T. and Grassberger, P., "A simple noise-reduction method for real data," Phys. Lett. A **160**, 411 (1991).

Smith, L. A., "Identification and prediction of low dimensional dynamics," Physica D **58**, 50 (1992).

Takens, F., "Detecting strange attractors in turbulence," Lect. Notes Math. **898**, 366 (1981).

Ueda, Y., "Randomly transitional phenomena in the system governed by Duffing's equation," J. Stat. Phys. **20**, 181 (1979).